THE JOURNAL OF BIOLOGICAL CHEMISTRY VOL. 287, NO. 20, pp. 16447–16453, May 11, 2012

Phosphatidylinositol 4,5-Bisphosphate Increases Ca^{2+} Affinity of Synaptotagmin-1 by 40-fold*

Received for publication, January 16, 2012, and in revised form, February 28, 2012 Published, JBC Papers in Press, March 23, 2012, DOI 10.1074/jbc.M112.343418

Geert van den Bogaart[‡1,2], **Karsten Meyenberg**[§1], **Ulf Diederichsen**[§], **and Reinhard Jahn**[‡3]

From the [‡]*Department of Neurobiology, Max Planck Institute for Biophysical Chemistry and the* [§]*Institute for Organic and Biomolecular Chemistry, Georg-August University, 37077 Göttingen, Germany*

Background: Synaptotagmin-1, a Ca^{2+} sensor of neuronal exocytosis, interacts with the anionic phospholipid phosphatidylinositol 4,5-bisphosphate (PIP_2).
Results: Microscale thermophoresis shows that PIP_2 binding to the polybasic patch of synaptotagmin-1 increases the Ca^{2+} affinity by >40-fold.
Conclusion: PIP_2 and Ca^{2+} binding to synaptotagmin-1 is strongly cooperative.
Significance: Understanding the interplay between Ca^{2+}, synaptotagmin-1, and PIP_2 is crucial for our understanding of neurotransmitter release.

Synaptotagmin-1 is the main Ca^{2+} sensor of neuronal exocytosis. It binds to both Ca^{2+} and the anionic phospholipid phosphatidylinositol 4,5-bisphosphate (PIP_2), but the precise cooperativity of this binding is still poorly understood. Here, we used microscale thermophoresis to quantify the cooperative binding of PIP_2 and Ca^{2+} to synaptotagmin-1. We found that PIP_2 bound to the well conserved polybasic patch of the C2B domain with an apparent dissociation constant of ~20 μM. PIP_2 binding reduced the apparent dissociation constant for Ca^{2+} from ~250 to <5 μM. Thus, our data show that PIP_2 makes synaptotagmin-1 >40-fold more sensitive to Ca^{2+}. This interplay between Ca^{2+}, synaptotagmin-1, and PIP_2 is crucial for neurotransmitter release.

In the synaptic terminal, neurotransmitter release is mediated by fusion of synaptic vesicles with the plasma membrane. Fusion is triggered by a sudden increase in the cytoplasmic Ca^{2+} concentration in response to membrane depolarization. The protein synaptotagmin-1 (together with synaptotagmin-2 and synaptotagmin-9) is the main Ca^{2+} sensor of the fast phase of neuronal exocytosis (reviewed in Ref. 1). Synaptotagmin-1 contains a single transmembrane domain close to the N terminus, which anchors the protein to synaptic vesicles. The transmembrane domain is connected by a 61-residue unstructured linker to two C2 domains, C2A and C2B. The mechanism by which synaptotagmin-1 triggers membrane fusion is still debated, but structural rearrangements of the plasma membrane and/or interactions with SNARE proteins have been implicated (1).

Ca^{2+} binding to synaptotagmin-1, originally demonstrated by equilibrium dialysis using native protein (2), has been characterized by isothermal titration calorimetry (3) and NMR (4–6) using a soluble fragment containing both C2 domains (C2AB fragment, residues 97–421). The C2A domain binds to three Ca^{2+} ions with affinities ranging from 50 μM to 10 mM. The C2B domain binds two Ca^{2+} ions, both with ~200 μM affinity.

In the presence of Ca^{2+}, the C2 domains of synaptotagmin-1 also bind to membranes containing anionic phospholipids, with little specificity for the phospholipid species (3, 6–14). Interestingly, binding already occurs at Ca^{2+} concentrations well below the Ca^{2+} affinity of free synaptotagmin-1. Here, anionic phospholipid headgroups complement the Ca^{2+}-binding sites, increasing the affinity of C2AB for Ca^{2+} to ~5–100 μM (3, 6–8, 11, 13). In the absence of Ca^{2+}, a conserved polybasic lysine patch located on the C2B domain can also bind to anionic lipids, and this binding is strongly preferential for the polyanionic phospholipid phosphatidylinositol 4,5-bisphosphate (PIP_2)[4] (3, 9–14). Binding of PIP_2 to the polybasic patch might increase the Ca^{2+} affinity (12), although this is still controversial (3) and has hitherto not been characterized in detail.

Experimentally, measuring synaptotagmin-1 binding to PIP_2 and/or Ca^{2+} is not trivial. Isothermal titration calorimetry and NMR require high (100 μM to 1 mM) concentrations of protein (3–5). Therefore, high affinities well below these concentrations cannot be accurately determined with these approaches. Binding of synaptotagmin to PIP_2 is often inferred from binding of the C2 domains to artificial membranes containing a defined fraction of PIP_2 (*e.g.* by FRET (3), pulldown assays (11, 13), or density flotations (3, 12)). However, it is difficult to quantitatively distinguish Ca^{2+} from PIP_2 binding with these approaches. We have recently shown (10) that Ca^{2+} binding to synaptotagmin-1 can be directly measured with a new technique called microscale thermophoresis (MST) (15, 16). MST is based on the principle that molecules move along a tempera-

* This work was supported, in whole or in part, by National Institutes of Health Grant P01 GM072694 (to R. J.) This work was also supported by Deutsche Forschungsgemeinschaft Grant SFB803.
[1] Both authors contributed equally to this work.
[2] Supported by the Human Frontier Science Program.
[3] To whom correspondence should be addressed: Dept. of Neurobiology, Max Planck Institute for Biophysical Chemistry, Am Faßberg 11, 37077 Göttingen, Germany. Tel.: 49-551-201-1635; Fax: 49-551-201-1639; E-mail: r.jahn@gwdg.de.

[4] The abbreviations used are: PIP_2, phosphatidylinositol 4,5-bisphosphate; MST, microscale thermophoresis.

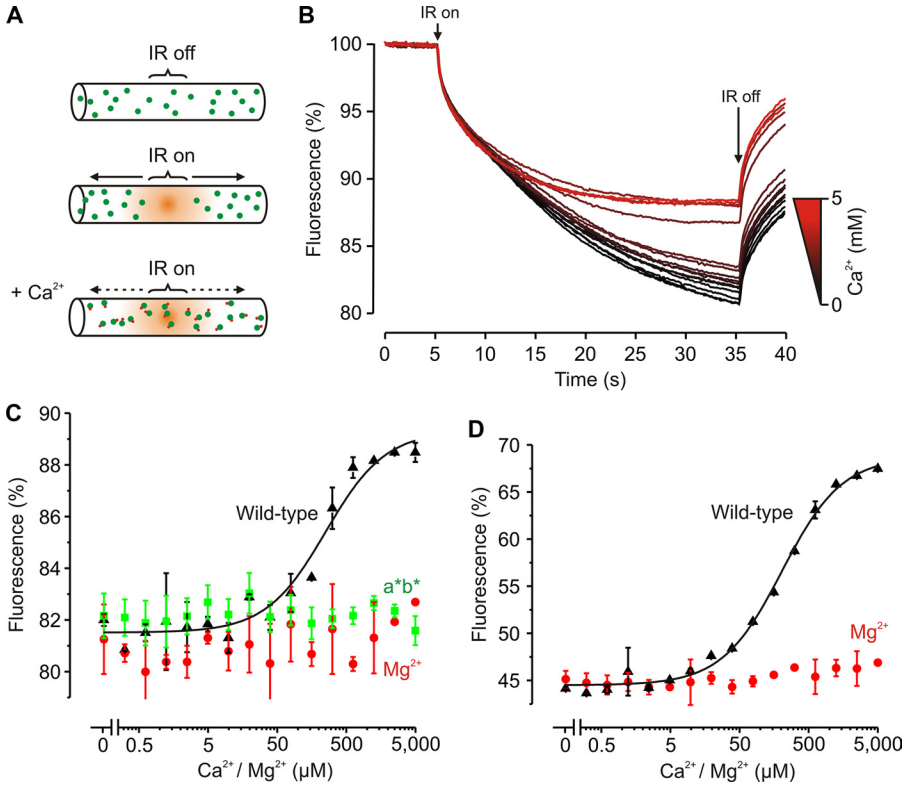

FIGURE 1. **Ca^{2+} binding to C2AB measured by MST.** *A*, principle of MST. A capillary containing 50 nM Alexa Fluor 488-labeled C2AB is locally heated by a focused IR laser (*IR on*). C2AB thermodiffuses away from the heated spot, causing a local depletion and a drop in fluorescence. Ca^{2+} binding changes the thermophoretic properties of C2AB, resulting in a decreased thermodiffusion. *B*, MST time traces of 16 different Ca^{2+} concentrations (ranging from 0 to 5 mM). Note that thermodiffusion is reduced at high Ca^{2+} concentrations. *C*, dependence of the MST signal on the Ca^{2+} concentration (measured 30 s after turning on heating; data from *B*). The *solid line* is a fit with Michaelis-Menten kinetics, yielding an apparent dissociation constant of $K_{Ca} = 221$ μM. No change in the MST signal was observed in the presence of Mg^{2+} or when a mutant impaired in Ca^{2+} binding was used (D178A/D230A/D232A/D309A/D363A/D365A, called C2a*b* (*a**b**)). *D*, same as *C* but using unlabeled C2AB. MST was measured using intrinsic tryptophan fluorescence and fitted, yielding $K_{Ca} = 206$ μM. *Error bars* indicate the range of data points obtained from at least two measurements.

ture gradient in a capillary (the Soret effect). Upon binding to Ca^{2+} or PIP_2, the surface properties of synaptotagmin-1 change, resulting in an altered thermophoretic behavior. In this study, we applied MST to study PIP_2 and Ca^{2+} cooperative binding to synaptotagmin-1.

EXPERIMENTAL PROCEDURES

The C2AB fragment of synaptotagmin-1 (rat sequence, residues 97–421) was expressed in *Escherichia coli* and purified as described (3, 10). The single cysteine mutant (C278S/S342C) was labeled with Alexa Fluor 488-maleimide (Invitrogen) as described (3, 10). Liposomes were prepared by extrusion of rehydrated lipid films through 100-nm pores (polycarbonate membranes, Avestin) (17). All lipids were from Avanti Polar Lipids. MST was measured with ~50 nM fluorescently labeled C2AB in 20 mM HEPES, 150 mM KCl, and 2.5 mg/ml BSA at pH 7.4. The samples were added to hydrophobic capillaries (NanoTemper Technologies), and MST was measured with a NanoTemper Monolith NT.015 system (25% light-emitting diode, 40% IR laser power). The label-free (tryptophan) experiments were performed with 1 μM wild-type C2AB, no BSA, and the NanoTemper Monolith NT.LabelFree instrument (80% UV light-emitting diode, 40% IR laser power). The MST curves were fitted with simple Michaelis-Menten kinetics to obtain the apparent dissociation constant for Ca^{2+} (K_{Ca}) or PIP_2 (K_{PIP2}). For Ca^{2+} binding, $T = A - B/(K_{Ca} + [Ca^{2+}])$, where T is the percentage of fluorescence after heating, $[Ca^{2+}]$ is the total calcium concentration in the capillary, and A and B are conversion factors for the thermophoresis.

RESULTS

We performed MST measurements on the Alexa Fluor 488-labeled C2AB fragment of synaptotagmin-1 (residues 97–421). With this technique, a glass capillary is filled with a dilute protein solution (50 nM). Fluorescence is then measured at a spot in the capillary that is heated with a focused IR laser beam. Heating (by ~5 °C) results in the generation of a temperature gradient along the axis of the capillary (Fig. 1, *A* and *B*). The C2AB fragment thermodiffuses out of this heated spot (measured by fluorescence recording), resulting in a protein gradient that is reversed when the IR laser is switched off. The amount of fluorescence decrease at the heated spot (the MST signal) was changed in the presence of Ca^{2+}, thus providing a direct readout of Ca^{2+} binding to the C2AB fragment. Evidently, Ca^{2+} binding alters the thermophoretic (*i.e.* surface, charge) properties and thereby the thermodiffusion of synaptotagmin (10). Varying the calcium concentration in the capillary thus allowed us to obtain a binding curve (Fig. 1*C*).

We fitted the binding curves with simple Michaelis-Menten kinetics assuming a single binding site (see "Experimental Procedures"). This model does not take into account binding of multiple Ca^{2+} ions (or PIP_2 molecules; see below), and for some

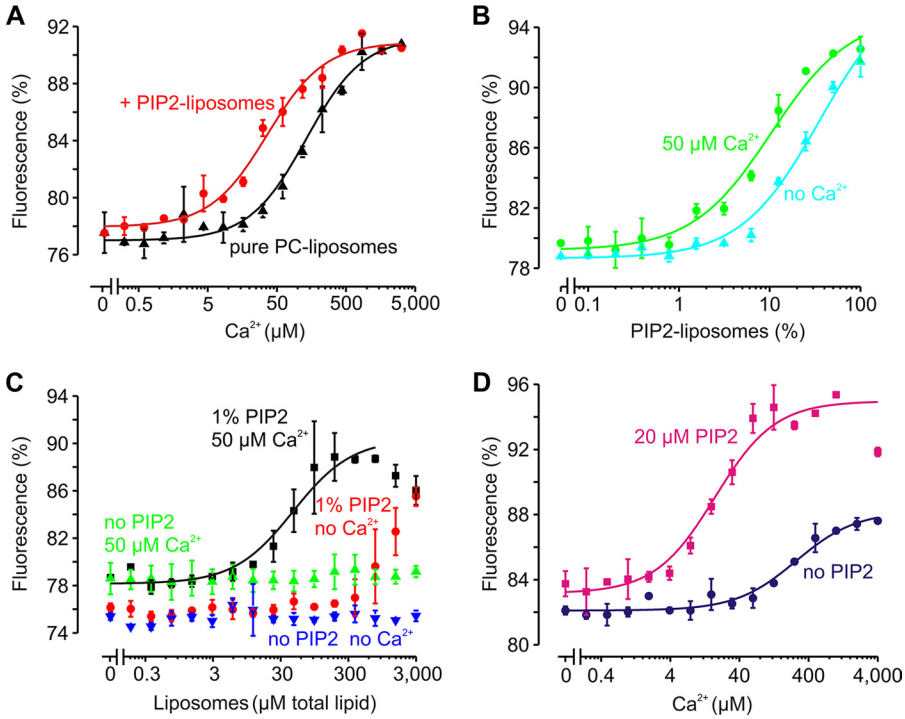

FIGURE 2. **Ca^{2+} dependence of MST signal of C2AB in presence of PIP_2-containing liposomes.** *A*, Ca^{2+} binding of the C2AB fragment in the presence of 1,2-dioleoyl-*sn*-glycero-3-phosphatidylcholine (*PC*)-containing liposomes (2.5 mM total lipid concentration) yielded an apparent dissociation constant of K_{Ca} = 226.7 ± 50.7 μM (*black*). However, when 10% of the 1,2-dioleoyl-*sn*-glycero-3-phosphatidylcholine-containing liposomes contained 5 mol % PIP_2, the affinity increased by ~5-fold to K_{Ca} = 46.0 ± 5.9 μM (*red*). *B*, liposome binding as a function of the fraction of PIP_2-containing liposomes. In all cases, the total lipid concentration was 2.5 mM, but the fraction of liposomes containing 5 mol % PIP_2 varied. In the absence of Ca^{2+}, C2AB bound to the PIP_2 membranes with K_{PIP2} = 36.2 ± 7.4% (or 45.3 μM PIP_2; *cyan*). In the presence of 50 μM Ca^{2+}, the affinity increased by 4-fold to K_{PIP2} = 10.6 ± 2.3% (or 13.3 μM PIP_2; *green*). *C*, binding of C2AB to liposomes composed of a 5:2:1:1 molar ratio of brain isolated phosphatidylcholine, phosphatidylethanolamine, phosphatidylserine, and cholesterol. C2AB did not bind to liposomes lacking PIP_2 regardless of the presence (*green*) or absence (*blue*) of 50 μM Ca^{2+}. In contrast, C2AB bound to liposomes containing 1 mol % PIP_2 already in the absence of Ca^{2+} (*red*). Similar to *B*, 50 μM Ca^{2+} increased the binding affinity (K_{PIP2} = 50.9 ± 20.0 μM total lipid concentration; *black*). *D*, Ca^{2+} binding curve of C2AB in the presence (K_{Ca} = 17.7 ± 0.7 μM; *pink*) or absence (K_{Ca} = 265.2 ± 27.4 μM; *blue*) of 20 μM PIP_2 in solution. 1 mM Mg^{2+} was present to suppress potentially unspecific Ca^{2+}-PIP_2 interactions. *Error bars* indicate the range of data points obtained from at least two measurements.

curves, this simplification may affect the quality of the fit. However, the overall quality of the data did not warrant fitting with a more sophisticated binding model. Thus, we could not differentiate between the different calcium-binding sites, and we report only the apparent dissociation constant (K_{Ca}).

C2AB bound to Ca^{2+} with K_{Ca} = 221 ± 23 μM (n = 3). Control experiments with Mg^{2+} or a mutant with disrupted Ca^{2+} binding (D178A/D230A/D232A/D309A/D363A/D365A, called C2a*b*) (3, 10) showed that the change in the MST signal was indeed due to binding of Ca^{2+} ions to the established binding sites in the C2 domains. Furthermore, the MST measurements were not affected by the presence of the dye because a similar binding constant of K_{Ca} = 206 ± 40 μM was obtained with the unlabeled C2AB fragment using the intrinsic tryptophan fluorescence as the readout (C2AB has three tryptophans) (Fig. 1*D*). We then set out to study the cooperativity of Ca^{2+} and PIP_2 binding.

No apparent change in the Ca^{2+}-dependent thermophoretic behavior of C2AB was observed in the presence of liposomes composed of pure 1,2-dioleoyl-*sn*-glycero-3-phosphatidylcholine (2.5 mM total lipid concentration; K_{Ca} = 226.7 ± 50.7 μM) (Fig. 2*A*). In contrast, the apparent affinity for Ca^{2+} increased by ~5-fold when only 10% of these liposomes were replaced with a liposome population composed of 95% 1,2-dioleoyl-*sn*-glycero-3-phosphatidylcholine and 5% PIP_2 (K_{Ca} = 46.0 ± 5.9 μM). Accordingly, the addition of 50 μM Ca^{2+} (well below the K_{Ca} of C2AB) resulted in ~4-fold stronger binding to PIP_2-containing liposomes (from K_{PIP2} = 45.3 ± 9.25 μM to 13.3 ± 2.9 μM total PIP_2 concentration) (Fig. 2*B*). 50 μM Ca^{2+} also increased C2AB binding to liposomes containing a more physiological lipid composition (phosphatidylcholine/phosphatidylethanolamine/phosphatidylserine/cholesterol at a molar ratio of 5:2:1:1) but only if 1 mol % PIP_2 was present (Fig. 2*C*). Thus, synaptotagmin-1 binds to anionic membranes and Ca^{2+} in a cooperative manner, as reported previously (3, 6–13). We performed a set of experiments with water-solubilized PIP_2 to further characterize this cooperativity.

One of the main advantages of MST compared with alternative techniques for measuring Ca^{2+} binding is the low concentration of protein that is required: measurements could be carried out with C2AB concentrations as low as 50 nM, which is 3–4 orders of magnitude below that reported for isothermal titration calorimetry (3) or NMR (4–6). This low concentration allowed us to measure PIP_2 binding by adding PIP_2 directly to the capillary (Fig. 2*D*). Even PIP_2 isolated from porcine brain with long fatty acid acyl chains (dominant species C18:0 and C20:4) is water-soluble at concentrations up to ~9 mM and does poorly form micelles because of its high anionic charge (18).

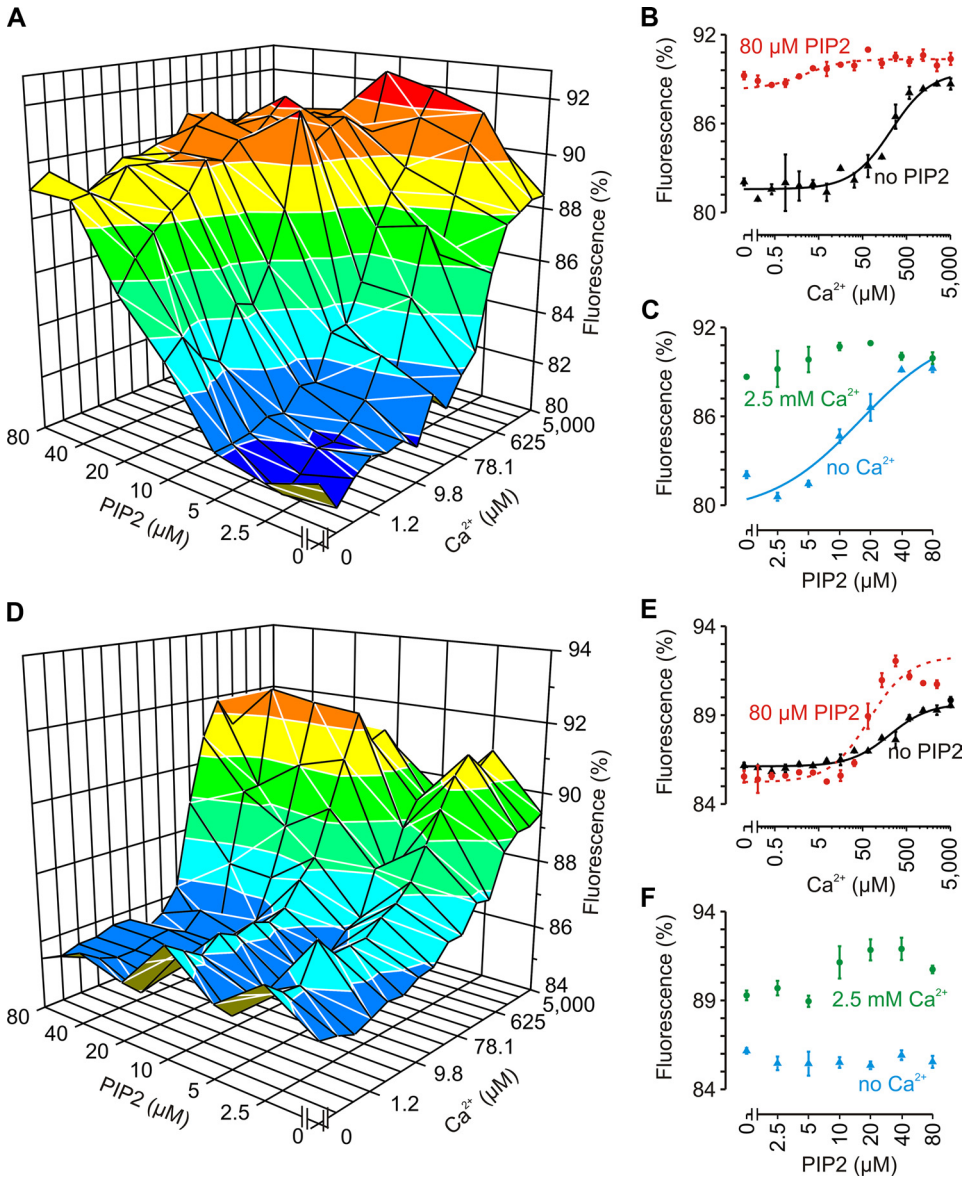

FIGURE 3. **Ca^{2+} and PIP_2 binding to C2AB measured by MST.** *A*, MST as a function of both Ca^{2+} and PIP_2. Each *x* and *y curve* (thus with the same Ca^{2+} or PIP_2 concentrations) was fitted with Michaelis-Menten kinetics to obtain the apparent dissociation constants (K_{Ca} and K_{PIP2}; see Fig. 4). *B*, two Ca^{2+} binding curves from *A* and their corresponding fits in the absence (K_{Ca} = 221 μM; *black*) or presence (K_{Ca} = 4.6 μM; *red*) of 80 μM PIP_2. *C*, two PIP_2 binding curves from *A* in the absence (K_{PIP2} = 20 μM; *blue*) or presence (KPIP2 < 5 μM; *green*) of 2.5 mM Ca^{2+}. *D–F*, same as *A–C* but for the KAKA mutant (K326A/K327A) (12). Compared with the wild type, the amplitude of the fluorescence changes of the KAKA mutant was reduced due to the altered thermophoretic properties that resulted from the substitution of charged residues. In *E*, the *solid* (no PIP_2) and *dashed* (80 μM PIP_2) lines are fits with K_{Ca} = 195 and 61 μM, respectively. Note that for the KAKA mutant, PIP_2 binding was dramatically reduced compared with the wild type. Each experiment was repeated at least twice; *error bars* show the range of data points.

Strikingly, the affinity for Ca^{2+} binding increased by 15-fold in the presence of 20 μM PIP_2 (from K_{Ca} = 265.2 ± 27.4 μM to 17.7 ± 0.7 μM) (Fig. 2*D*). In this experiment, an excess of 1 mM Mg^{2+} was present to suppress potential nonspecific interactions of Ca^{2+} with PIP_2 or C2AB. At higher PIP_2 concentrations, the Ca^{2+} affinity increased even further (to >40-fold; K_{Ca} = 3.3 ± 1.3 μM at 40–80 μM PIP_2 compared with 221 ± 23 μM without PIP_2) (Fig. 3, *A–C*). Accordingly, the addition of Ca^{2+} progressively increased the binding affinity of C2AB for PIP_2 (from K_{PIP2} = 20 ± 5 μM without Ca^{2+} to <2 μM at >20 μM Ca^{2+}). This cooperativity is not specific for PIP_2 or the length of the acyl chains because another phosphoinositide (20 μM phosphatidylinositol 3,5-bisphosphate) or short-chain PIP_2 (20 μM 1,2-dioctanoyl-*sn*-glycero-3-phosphatidylinositol 4′,5′-bisphosphate; C8:0) also increased the apparent Ca^{2+} affinity (K_{Ca} = 11 ± 5 and 8 ± 5 μM, respectively).

PIP_2 binding required the well conserved polybasic patch that is located on the C2B domain because removal of two lysines from this patch (K326A/K327A, the so-called KAKA mutant (12)) (Fig. 3, *D–F*, and Fig. 4, *A* and *B*) almost completely abolished PIP_2-dependent MST changes, even at very high Ca^{2+} concentrations. Accordingly, the apparent affinity for Ca^{2+} was increased by only ~3-fold in the presence of 80 μM PIP_2 (from K_{Ca} = 195 ± 35 μM to 61 ± 11 μM). Thus, we could detect only PIP_2 binding to the polybasic patch and did not observe PIP_2 binding via the Ca^{2+}-binding sites on the C2A

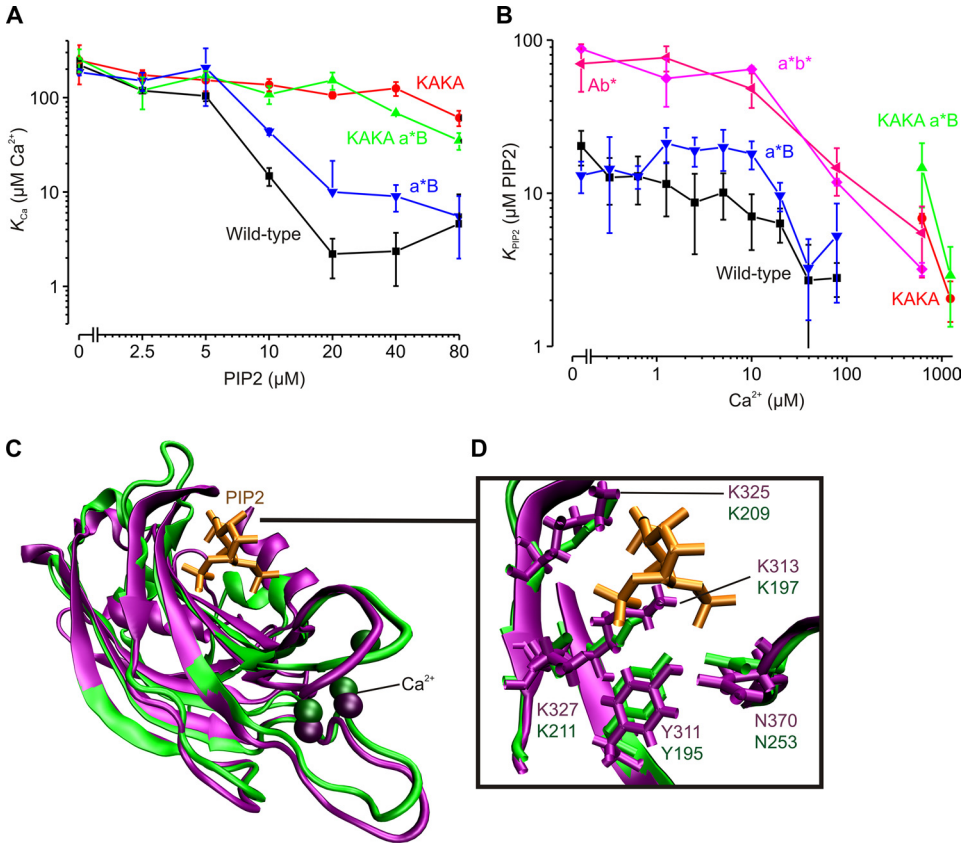

FIGURE 4. **Cooperative Ca^{2+} and PIP_2 binding to C2AB.** The apparent dissociation constants for Ca^{2+} binding (K_{Ca}; *A*) and PIP_2 binding (K_{PIP2}; *B*) were determined by MST. Wild-type C2AB (see Fig. 3, *A–C*) and various mutants were tested: KAKA (K326A/K327A; see Fig. 3, *D–F*), C2a*B (*a*B*; D178A/D230A/D232A), C2Ab* (*Ab**; D309A/D363A/D365A), C2a*b* (*a*b**; D178A/D230A/D232A/D309A/D363A/D365A), and KAKA/C2a*B (*KAKA a*B*). The KAKA/C2Ab* and KAKA/C2a*b* mutants are not shown in the figure because PIP_2 and Ca^{2+} binding could not be detected with MST (see Fig. 1*C*). *Error bars* show the range of data points obtained from at least two measurements. *C*, conservation of the PIP_2-binding sites. The crystal structure of the C2B domain (*purple*; Protein Data Bank code 1TJX (26)) was overlapped with that of the PIP_2-bound PKCα C2 domain (*green*; code 3GPE (25)). *D*, all residues that stabilize the PIP_2 headgroup (*orange*) are conserved in the C2B domain (see also Ref. 25).

and C2B domains, in contrast to previous observations by us and others (3, 10–12, 14). It is likely that, for the interaction of the Ca^{2+}-binding pockets with the membrane, hydrophobic residues surrounding these pockets must insert into the membrane (6–8, 11, 12, 14), although we cannot exclude that PIP_2 binding to the Ca^{2+} sites is silent (*i.e.* does not change the MST signal). Nevertheless, the Ca^{2+}-binding pocket of the C2B domain does affect PIP_2 binding to the polybasic patch because disruption of Ca^{2+} binding to the C2B domain (D309A/D363A/D365A, called C2Ab*) reduced the affinity for PIP_2 by ~4-fold (from $K_{PIP2} = 20.4 \pm 5.2$ μM to 70 ± 24 μM) (Fig. 4*B*).

We then performed MST experiments with mutants disrupted in Ca^{2+} binding to the C2A domain (D178A/D230A/D232A, called C2a*B). Surprisingly, only a small and insignificant PIP_2- or Ca^{2+}-dependent change in the MST signal of C2a*B was observed compared with the wild type (Fig. 4, *A* and *B*). Accordingly, the combination of C2a*B with the KAKA mutation did not markedly differ from the KAKA mutant with all Ca^{2+}-binding sites intact. Apparently, Ca^{2+} binding to the C2A domain does not result in a detectable change in the thermophoretic properties of the C2AB fragment. In contrast, Ca^{2+} binding could no longer be detected by MST upon disruption of the C2B domain. Thus, only Ca^{2+} binding to the C2B domain seems to change the thermophoretic properties of the C2AB fragment, indicating that the calcium-dependent changes reported above are exclusively mediated by the C2B domain. Perhaps this selectivity is related to the thermodynamically divergent modes of Ca^{2+} binding of synaptotagmin-1: Ca^{2+} binding to the C2A domain is endothermic, and that to the C2B domain is exothermic (3). Finally, Ca^{2+} concentrations above 100 μM increased the apparent PIP_2 affinity of synaptotagmin-1 even when both Ca^{2+}-binding sites were disrupted (double mutant C2a*b*) (Fig. 4*B*). This indicates that Ca^{2+} was still able to bind to the double mutant at very high Ca^{2+} concentrations in the presence of PIP_2, perhaps by binding directly to PIP_2 (19, 20).

DISCUSSION

In this work, we have shown that PIP_2 binds to the polybasic patch of the C2B domain of synaptotagmin-1, in agreement with earlier studies (10–14, 21). PIP_2 binding to the polybasic patch increases the apparent affinity of the C2B domain for Ca^{2+} by >40-fold. Conversely, Ca^{2+} binding to the C2B domain increases the affinity for PIP_2 by >10-fold. Cooperative PIP_2 and Ca^{2+} binding to synaptotagmin-1 has been observed previously (12). This cooperativity is probably not caused by complementation of the Ca^{2+}-binding sites, as suggested earlier by us and others (3, 6–8), because the polybasic patch and

the Ca^{2+}-binding sites are located quite far apart (Fig. 4*C*). Instead, PIP_2 may interact in a structurally less defined manner with the polybasic patch and other solvent-exposed basic residues (9, 12), and this may increase the Ca^{2+} affinity simply by charge screening. Alternatively, the polybasic patch may form a structurally defined complex with PIP_2 similar to the C2 domains of rabphilin-3A and PKCα (22–25). In fact, cooperative PIP_2 and Ca^{2+} binding has been observed for these C2 domains (22–24), very similar to our observations for the C2B domain. Moreover, the crystal structure of the C2B domain (26) can be superimposed with that of the PIP_2-bound C2 domain of PKCα (25), rendering it likely that PIP_2 binds to the C2AB fragment of synaptotagmin-1 in a similar manner (Fig. 4, *C* and *D*). Thus, it is conceivable that such PIP_2 binding increases the Ca^{2+} affinity via a conformational change. However, how PIP_2 and Ca^{2+} precisely bind in a cooperative manner to synaptotagmin-1 remains to be elucidated.

Together, we conclude that PIP_2 binding to the polybasic patch of synaptotagmin-1 dramatically increases the Ca^{2+} sensitivity. As discussed previously (12), this explains the reduced release probability of the KAKA mutant in hippocampal neurons (12, 27) and in *Drosophila* (28). It also explains why *in vivo* already 10 μM Ca^{2+} is sufficient for physiological release of neurotransmitters in the calyx of Held (29). PIP_2 modulation of synaptotagmin-1 may well be of major physiological relevance when considering that PIP_2 is the predominant phospholipid species at the sites of docked vesicles in PC12 cells (30).

Finally, our work demonstrates the value of MST for measuring molecular interactions. Although we were unable to detect Ca^{2+} binding to the C2A domain under our conditions, MST can be extremely sensitive and allows for monitoring medium and high affinity interactions with only picomoles of material. MST has the potential to complement the limited set of techniques available to measure Ca^{2+} and PIP_2 binding to proteins under equilibrium conditions such as isothermal titration calorimetry and NMR.

Acknowledgment—We thank Stefan Duhr (NanoTemper Technologies GmbH) for advice and the label-free measurements.

REFERENCES

1. Chapman, E. R. (2008) How does synaptotagmin trigger neurotransmitter release? *Annu. Rev. Biochem.* **77,** 615–641
2. Brose, N., Petrenko, A. G., Südhof, T. C., and Jahn, R. (1992) Synaptotagmin: a calcium sensor on the synaptic vesicle surface. *Science* **256,** 1021–1025
3. Radhakrishnan, A., Stein, A., Jahn, R., and Fasshauer, D. (2009) The Ca^{2+} affinity of synaptotagmin-1 is markedly increased by a specific interaction of its C2B domain with phosphatidylinositol 4,5-bisphosphate. *J. Biol. Chem.* **284,** 25749–25760
4. Ubach, J., Zhang, X., Shao, X., Südhof, T. C., and Rizo, J. (1998) Ca^{2+} binding to synaptotagmin: how many Ca^{2+} ions bind to the tip of a C2 domain? *EMBO J.* **17,** 3921–3930
5. Fernandez, I., Araç, D., Ubach, J., Gerber, S. H., Shin, O., Gao, Y., Anderson, R. G., Südhof, T. C., and Rizo, J. (2001) Three-dimensional structure of the synaptotagmin-1 C2B domain: synaptotagmin-1 as a phospholipid-binding machine. *Neuron* **32,** 1057–1069
6. Fernández-Chacón, R., Königstorfer, A., Gerber, S. H., García, J., Matos, M. F., Stevens, C. F., Brose, N., Rizo, J., Rosenmund, C., and Südhof, T. C. (2001) Synaptotagmin-1 functions as a calcium regulator of release probability. *Nature* **410,** 41–49
7. Davletov, B. A., and Südhof, T. C. (1993) A single C2 domain from synaptotagmin-1 is sufficient for high affinity Ca^{2+}/phospholipid binding. *J. Biol. Chem.* **268,** 26386–26390
8. Zhang, X., Rizo, J., and Südhof, T. C. (1998) Mechanism of phospholipid binding by the C2A domain of synaptotagmin-1. *Biochemistry* **37,** 12395–12403
9. Araç, D., Chen, X., Khant, H. A., Ubach, J., Ludtke, S. J., Kikkawa, M., Johnson, A. E., Chiu, W., Südhof, T. C., and Rizo, J. (2006) Close membrane-membrane proximity induced by Ca^{2+}-dependent multivalent binding of synaptotagmin-1 to phospholipids. *Nat. Struct. Mol. Biol.* **13,** 209–217
10. van den Bogaart, G., Thutupalli, S., Risselada, J. H., Meyenberg, K., Holt, M., Riedel, D., Diederichsen, U., Herminghaus, S., Grubmüller, H., and Jahn, R. (2011) Synaptotagmin-1 may be a distance regulator acting upstream of SNARE nucleation. *Nat. Struct. Mol. Biol.* **18,** 805–812
11. Bai, J., Tucker, W. C., and Chapman, E. R. (2004) PIP_2 increases the speed of response of synaptotagmin and steers its membrane penetration activity toward the plasma membrane. *Nat. Struct. Mol. Biol.* **11,** 36–44
12. Li, L., Shin, O. H., Rhee, J. S., Araç, D., Rah, J. C., Rizo, J., Südhof, T., and Rosenmund, C. (2006) Phosphatidylinositol phosphates as coactivators of Ca^{2+} binding to C2 domains of synaptotagmin-1. *J. Biol. Chem.* **281,** 15845–15852
13. Schiavo, G., Gu, Q. M., Prestwich, G. D., Söllner, T. H., and Rothman, J. E. (1996) Calcium-dependent switching of the specificity of phosphoinositide binding to synaptotagmin. *Proc. Natl. Acad. Sci. U.S.A.* **93,** 13327–13332
14. Kuo, W., Herrick, D. Z., and Cafiso, D. S. (2011) Phosphatidylinositol 4,5-bisphosphate alters synaptotagmin-1 membrane docking and drives opposing bilayers closer together. *Biochemistry* **50,** 2633–2641
15. Wienken, C. J., Baaske, P., Rothbauer, U., Braun, D., and Duhr, S. (2010) Protein binding assays in biological liquids using microscale thermophoresis. *Nat. Commun.* **1,** 100
16. Duhr, S., and Braun, D. (2006) Why molecules move along a temperature gradient. *Proc. Natl. Acad. Sci. U.S.A.* **103,** 19678–19682
17. van den Bogaart, G., Mika, J. T., Krasnikov, V., and Poolman, B. (2007) The lipid dependence of melittin action investigated by dual-color fluorescence burst analysis. *Biophys. J.* **93,** 154–163
18. Chu, A., and Stefani, E. (1991) Phosphatidylinositol 4,5-bisphosphate-induced Ca^{2+} release from skeletal muscle sarcoplasmic reticulum terminal cisternal membranes. Ca^{2+} flux and single channel studies. *J. Biol. Chem.* **266,** 7699–7705
19. Carvalho, K., Ramos, L., Roy, C., and Picart, C. (2008) Giant unilamellar vesicles containing phosphatidylinositol 4,5-bisphosphate: characterization and functionality. *Biophys. J.* **95,** 4348–4360
20. Levental, I., Christian, D. A., Wang, Y. H., Madara, J. J., Discher, D. E., and Janmey, P. A. (2009) Calcium-dependent lateral organization in phosphatidylinositol 4,5-bisphosphate (PIP_2)- and cholesterol-containing monolayers. *Biochemistry* **48,** 8241–8248
21. Fukuda, M., Kojima, T., Aruga, J., Niinobe, M., and Mikoshiba, K. (1995) Functional diversity of C2 domains of synaptotagmin family. Mutational analysis of inositol high polyphosphate-binding domain. *J. Biol. Chem.* **270,** 26523–26527
22. Montaville, P., Coudevylle, N., Radhakrishnan, A., Leonov, A., Zweckstetter, M., and Becker, S. (2008) The PIP_2 binding mode of the C2 domains of rabphilin-3A. *Protein Sci.* **17,** 1025–1034
23. Torrecillas, A., Laynez, J., Menéndez, M., Corbalán-García, S., and Gómez-Fernández, J. C. (2004) Calorimetric study of the interaction of the C2 domains of classical protein kinase C isoenzymes with Ca^{2+} and phospholipids. *Biochemistry* **43,** 11727–11739
24. Guerrero-Valero, M., Marín-Vicente, C., Gómez-Fernández, J. C., and Corbalán-García, S. (2007) The C2 domains of classical PKCs are specific PtdIns(4,5)P_2-sensing domains with different affinities for membrane binding. *J. Mol. Biol.* **371,** 608–621
25. Guerrero-Valero, M., Ferrer-Orta, C., Querol-Audí, J., Marin-Vicente, C., Fita, I., Gómez-Fernández, J. C., Verdaguer, N., and Corbalán-García, S. (2009) Structural and mechanistic insights into the association of PKCα C2

domain with PtdIns(4,5)P_2. *Proc. Natl. Acad. Sci. U.S.A.* **106,** 6603–6607
26. Cheng, Y., Sequeira, S. M., Malinina, L., Tereshko, V., Söllner, T. H., and Patel, D. J. (2004) Crystallographic identification of Ca^{2+} and Sr^{2+} coordination sites in synaptotagmin-1 C2B domain. *Protein Sci.* **13,** 2665–2672
27. Borden, C. R., Stevens, C. F., Sullivan, J. M., and Zhu, Y. (2005) Synaptotagmin mutants Y311N and K326A/K327A alter the calcium dependence of neurotransmission. *Mol. Cell. Neurosci.* **29,** 462–470
28. Mackler, J. M., and Reist, N. E. (2001) Mutations in the second C2 domain of synaptotagmin disrupt synaptic transmission at *Drosophila* neuromuscular junctions. *J. Comp. Neurol.* **436,** 4–16
29. Schneggenburger, R., and Neher, E. (2005) Presynaptic calcium and control of vesicle fusion. *Curr. Opin. Neurobiol.* **15,** 266–274
30. van den Bogaart, G., Meyenberg, K., Risselada, H. J., Amin, H., Willig, K. I., Hubrich, B. E., Dier, M., Hell, S. W., Grubmüller, H., Diederichsen, U., and Jahn, R. (2011) Membrane protein sequestering by ionic protein-lipid interactions. *Nature* **479,** 552–555